Full Paper

Periodic mesoporous organosilica grafted palladium organometallic complex: efficient heterogeneous catalyst for water-medium organic reactions

Jianlin Huang and Fang Zhang*

Water-medium organic reactions were studied over periodic mesoporous silica (PMO) containing Pd(II) organometallic complex. This heterogeneous catalyst was achieved by Pd(II) compound coordinated with the PPh_2-ligand onto the pore surface of phenylene-bridged PMO support. This catalyst displayed ordered mesoporous channels, which ensured the high dispersion of Pd(II) active sites and the convenient diffusion of reactant molecules into the pore channels. Meanwhile, the phenyl group in the pore wall of PMO could enhance the surface hydrophobicity which promoted the adsorption of organic reactant molecules on the catalyst in aqueous environment. As a result, this elaborated catalyst exhibited comparable activity and selectivity with the corresponding $PdCl_2(PPh_3)_2$ homogeneous catalyst in the water-medium organic reactions, and could be used repeatedly, showing a good potential in industrial applications. Copyright © 2010 John Wiley & Sons, Ltd.

Keywords: periodic mesoporous silica; heterogeneous catalyst; water-medium; $PdCl_2(PPh_3)_2$; immobilization

Introduction

In nature, numerous biological processes occur in aqueous environments with unparalleled catalytic activity and selectivity.[1] In contrast, scientists require the aid of toxic, volatile organic solvents to complete synthetic procedures, which inevitably risks environmental pollution and human health problems.[2] Accordingly, increasing social pressure is requiring scientists to find green chemical processes that can be conducted in water. The use of water as a solvent in organic reactions offers significant environmental advantages because water is the cleanest and safest solvent.[3] Many organic reactions have been facilitated in aqueous media with satisfactory activity and selectivity. However, most of them are performed by homogeneous catalysts, which usually have disadvantages in separation and recycling, thus adding to the cost and even causing environmental pollution by heavy metallic ions.[4]

The alternative approach for water-medium chemical transformations is immobilized heterogeneous catalysts.[5] Although the efficiency of heterogeneous catalysis is generally inferior to that of homogeneous systems, the advantages of this kind of catalyst include their easy recovery from reaction mixtures and their reusability. The major dilemma for the heterogeneous catalytic system is the limited solubility of most organic molecules in water.[6] We and other groups employed the functionalized mesoporous silica as a support to address the above limitation. It was found that the functionalization of silica support with organic groups could strengthen the surface hydrophobicity, which facilitated the adsorption of organic reactants on the catalyst, leading to the enhanced activity and selectivity.[7,8] However, the incorporation of the organic groups in the pore channels might limit the diffusion of reactant molecules due to the blockage of pore channels, which is unfavorable for cat-

alytic activity. Meanwhile, the organic groups anchoring on the pore surface might easily leach off during liquid phase catalysis, leading to poor catalyst durability.[9] The recent discovery of the periodic mesoporous organosilicas (PMOs), built from bridged organosilane precursors, wherein organic group R is an integral part of the mesoporous wall, opened up a new avenue for organo-modified mesoporous materials. Unlike organic group-functionalized mesoporous silicas, the organic groups are homogeneously distributed in the framework of PMOs, which could provide a novel platform for water-medium organic reactions in a designated way by altering the pore structure and chemical composition.[10]

In this work, we report a facile approach to a novel Pd(II) organometallic catalyst immobilized on a phenylene-bridged PMO support. As expected, this catalyst exhibited superiority over other heterogeneous catalysts and even equivalent catalytic efficiency to homogeneous catalysts during aqueous organic reactions. Furthermore, this heterogeneous catalyst can be reused at least five times with only slight loss of catalytic activity.

Experimental

Catalyst Preparation

The diphenylphosphine-functionalized phenylene (Ph)-bridged PMO was prepared via co-condensation of bis(triethoxysilyl)

* Correspondence to: Fang Zhang, Department of Chemistry, Shanghai Normal University, 100 Guilin Road, Shanghai 200234, China.
E-mail: zhangfang@shnu.edu.cn

Department of Chemistry, Shanghai Normal University, 100 Guilin Road, Shanghai 200234, China

benzene (BTESB) and 2-(diphenylphosphino) ethyltriethoxysilane (DPPES), denoted as PPh_2–PMO–Ph. In a typical synthesis, 1.0 g P123 and 3.0 g KCl were dissolved in 40 ml 0.067 M HCl aqueous solution and stirred for 2 h, followed by adding 1.0 g BTESB and 0.21 g DPPES. After stirring for 24 h at 313 K, the mixture was transferred into an autoclave and allowed hydrothermal treatment at 373 K for another 24 h. The molar ratio of organosilane : P123 : KCl : HCl : H_2O in the mixture was 1.0 : 0.034 : 7.8 : 2.43 : 415. The white solid product was recovered by filtration and dried in vacuum, followed by extraction in 500 ml ethanol solution at 353 K for 24 h to remove surfactant molecules and other adsorbed organic residues.

The Pd(II) organometallic catalyst immobilized on the PPh_2–PMO–Ph support was prepared by coordinating Pd(II) ions with the PPh_2-ligand. Briefly, 1.0 g PPh_2–PMO–Ph was added to 30 ml toluene solution containing 0.20 g $PdCl_2(PPh_3)_2$ and stirred for 12 h at room temperature under an argon atmosphere. The yellow solid was washed with toluene until the filtrate became colorless, followed by Soxlet-extraction with dichloromethane to remove Pd(II) species that physisorbed on the support. The final catalyst (Pd–PPh_2–PMO–Ph) with a Pd(II) loading of 1.1 wt% was dried under vacuum at 353 K. For comparison, both the PPh_2–SBA-15 and the PPh_2–SBA-15–Ph were prepared according to the method reported previously.[7,8] The Pd(II) organometallic complex was immobilized on these two supports in the same way as described above, and the as-prepared catalysts were denoted as Pd–PPh_2–SBA-15 and Pd–PPh_2–SBA-15–Ph, respectively.

Characterization

The Pd(II) loading was determined by inductively coupled plasma optical emission spectrometer (ICP, Varian VISTA-MPX). The X-ray powder diffraction (XRD) patterns were recorded on a Rigaku D/Max-RB diffractometer with CuK_α radiation. Morphologies were observed by transmission electron microscopy (TEM, Jeol JEM2010). Fourier transform infrared (FTIR) spectra were collected with a Nicolet Magna 550 spectrometer by using the KBr method. N_2 adsorption isotherms were measured at 77 K using a Quantachrome Nova 4000e analyzer after being outgassed at 373 K overnight. The specific surface area (S_{BET}), average pore diameter (D_P) and pore volume (V_P) were calculated based on BET method and BJH model, respectively. Solid-state NMR spectra were obtained on a Bruker AV-400 instrument. Thermal gravimetric analysis (TGA) was performed with a Perkin-Elmer Pyris Diamond TG analyzer under an air atmosphere with a heating ramp of 10 K/min. The surface electronic states were analyzed by X-ray photoelectron spectroscopy (XPS, PHI5000 versa probe). All the binding energy values were calibrated using $C_{1S} = 284.8$ eV as a reference.

Activity Test

The Barbier reactions were carried out at 323 K in a 25 ml round-bottomed flask. In a typical run, a catalyst containing 0.051 mmol Pd, 0.050 ml benzaldehyde, 0.20 ml allyl bromide, 5.0 ml distilled water and 0.45 g $SnCl_2$ were mixed and allowed to react for 12 h under reflux. Then the solution was extracted by ether and dried by $MgSO_4$, followed by filtrating solid catalyst and evaporating solvent. Reaction products were quantitatively analyzed on a gas chromatograph (GC, Agilent 1790) equipped with an FID and a JWDB-5 95% dimethyl 1-(5%)-diphenylpolysiloxane column
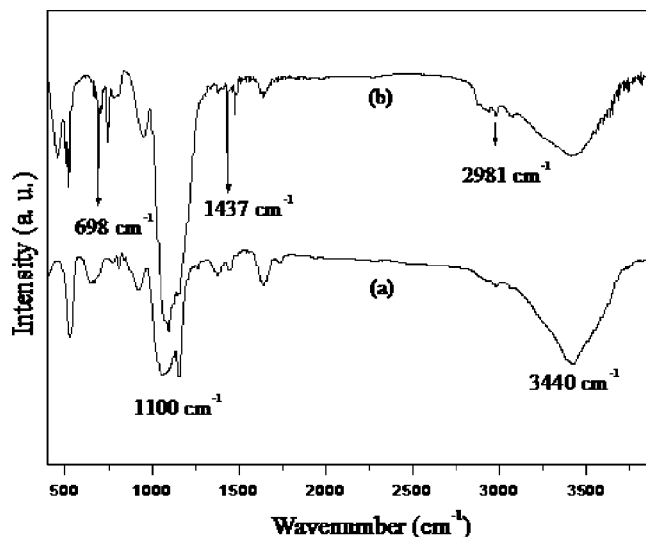

Figure 1. IR spectra of (a) the PMO-Ph and (b) the PPh_2-PMO-Ph samples.

at 373 K in N_2 flow, from which both the reaction conversion and the selectivity were calculated using internal standards. The reproducibility was checked by repeating each result at least three times and was found to be within acceptable limits (±5%).

In order to determine the catalyst durability, the Pd–PPh_2–PMO–Ph catalyst was allowed to settle down after each run of reactions and the clear supernatant liquid was decanted slowly. After being washed with toluene, the catalyst was re-used with fresh charge of solvent and reactant for subsequent reaction under the same conditions. The content of Pd species leached off from the heterogeneous catalyst was determined by ICP analysis.

Results and Discussion

Characterizations of Catalysts

The FTIR spectra (Fig. 1) revealed that, in comparison with the PMO–Ph, the PPh_2–PMO–Ph displayed three additional absorbance bands around 2981, 698 and 1437 cm^{-1}, indicative of the asymmetric and symmetric stretching modes of the C–H bond[11] and the -H out-of-plane deformation of the monosubstituted benzene ring as well as the vibration from the P–C bond, showing the successful incorporation of the PPh_2-CH_2-CH_2- groups into the PMO–Ph support.[12] These groups replaced the surface OH- groups, leading to considerable decrease in the absorbance at 3440 cm^{-1} characteristic of Si-OH groups. The P–Ph vibration band was normally observed in the range from 1090 to 1130 cm^{-1}, which could not be resolved due to the overlap by the intense peak resulted from the Si–O vibration.

As shown in Fig. 2, the XPS spectra demonstrated that all the Pd species in the Pd–PPh_2–PMO–Ph sample were present in bivalence state, corresponding to the binding energy (BE) of 337.3 eV in the $Pd_{3d5/2}$ level. In comparison with the BE of the Pd(II) in $Pd(PPh_3)_2Cl_2$,[13] the BE of the Pd(II) in Pd–PPh_2–PMO–Ph shifted negatively by 0.70 eV, which was could attributed to the stronger electron-donation ability of the PPh_2–CH_2-CH_2–ligand to the Pd(II) than that of the PPh_3–ligand. This could be easily

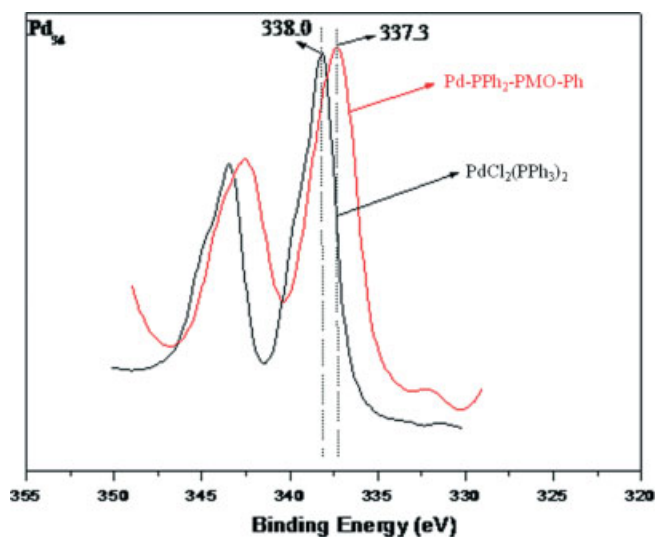**Figure 2.** XPS spectra of the Pd(PPh$_3$)$_2$Cl$_2$ and the Pd-PPh$_2$-PMO-Ph samples.

understood by considering the conjugated $\pi-\pi$ system between P and Ph, which could dilute the electron density on the P atom.[14] Thus, it could be concluded that Pd(II) complex was anchored onto the PMO support by the coordinated bonding approach (Scheme 1).

Figure 3 shows solid-state NMR spectra of the Pd–PPh$_2$–PMO–Ph sample. The ^{29}Si MAS NMR spectrum displayed three resonance peaks up-field corresponding to T^3 ($\delta = -81$ ppm), T^2 ($\delta = -72$ ppm) and T^1 ($\delta = -63$ ppm), where T^m = RSi(OSi)$_m$–(OH)$_{3-m}$ ($m = 1$–3). No Q^n peaks are observed, where Q^n = Si(OSi)$_n$–(OH)$_{4-n}$ ($n = 2$–4) suggesting that all the Si species were covalently bonded with carbon atoms.[15] From the ^{13}C CP-MAS NMR spectrum, one could see two peaks around 13 and 33 ppm, attributed to two C atoms in the PPh$_2$-CH$_2$-CH$_2$-group. Meanwhile, an intense peak around 138 ppm was assigned to the C atoms in the benzene ring.[16] The peak at 58 ppm was assigned to the C atoms in the C$_2$H$_5$O group connected with Si due to the incomplete hydrolysis.[17] Other peaks denoted by asterisks were attributed to rotational sidebands.[18] No significant resonance peaks in the range of 67–77 ppm were observed, implying the complete removal of P123 surfactant in the Pd–PPh$_2$–PMO–Ph sample. Meanwhile, the ^{31}P MAS NMR spectrum displayed a strong peak at 21.4 ppm and a shoulder peak around 24.3 ppm, which could be assigned to two kinds of P atoms in the Pd(II)–PPh$_2$ and the
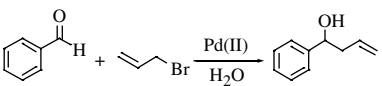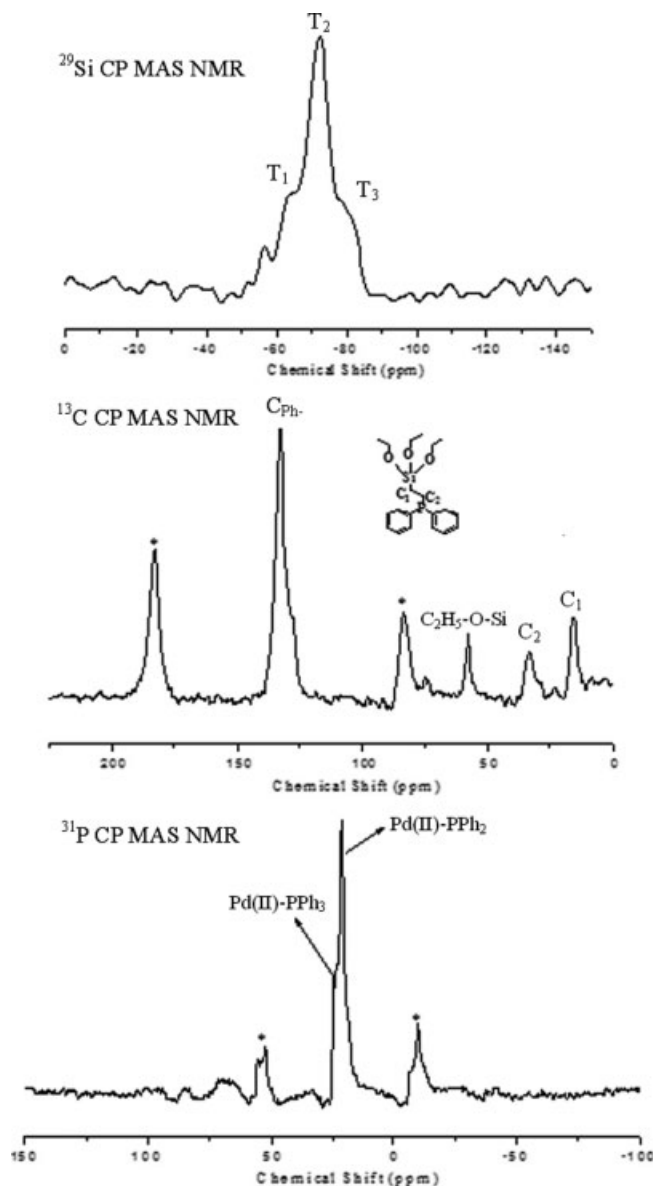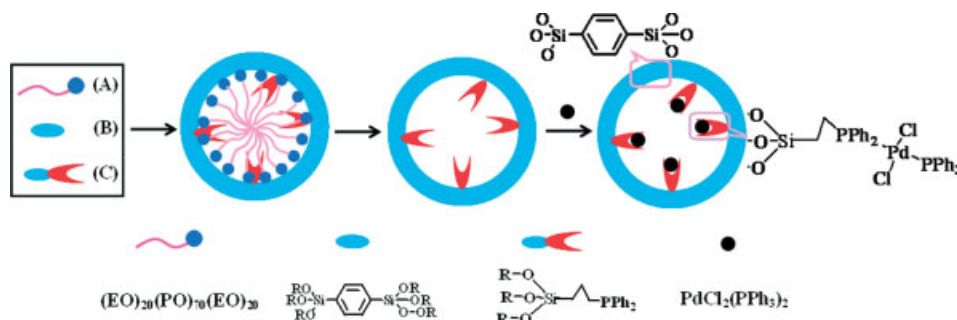

**Figure 3.** Solid state NMR spectra of the Pd-PPh$_2$-PMO-Ph sample.

Scheme 1. Schematic image of the formation of Pd-PPh$_2$-PMO-Ph catalyst.

Table 1. Structural properties and catalytic performances of different Pd(II) organometallic catalysts[a]

Catalyst	Pd loading (wt%)	S_{BET} (m^2/g)	D_P (nm)	V_P (cm^3/g)	Conversion (%)	Selectivity (%)	Yield (%)
PPh$_2$–PMO–Ph	–	777	4.2	0.78	–	–	–
Pd–PPh$_2$–PMO–Ph	1.1	538	3.6	0.48	92	92	84
Pd–PPh$_2$–SBA-15–Ph	0.50	184	1.9	0.15	76	94	71
Pd–PPh$_2$–SBA-15	0.60	389	5.1	0.57	54	89	41
Pd–PPh$_2$–PMO–Ph[b]	0.90	145	1.7	0.10	64	89	57

[a] Reaction conditions: a catalyst containing 0.051 mmol Pd(II), 0.050 ml benzaldehyde, 0.20 ml allyl bromide, 0.25 mmol 2-phenylethanol as internal standard, 5.0 ml H$_2$O, 2.0 mmol SnCl$_2$, reaction temperature = 323 K, reaction time = 12 h. The conversion was calculated by benzaldehyde.
[b] The catalyst after being used repetitively six times.
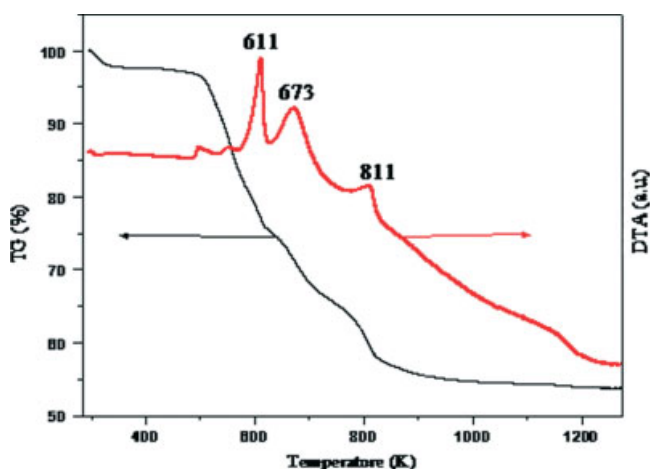
Figure 4. TG and DTA curves of the Pd-PPh$_2$-PMO-Ph sample.
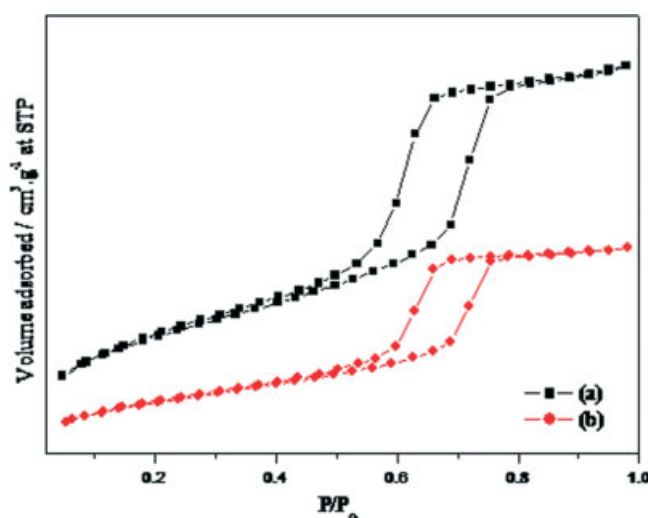
Figure 5. N$_2$ adsorption-desorption isotherms of (a) the PPh$_2$-PMO-Ph and (b) the Pd-PPh$_2$-PMO-Ph samples.

Pd(II)–PPh$_3$ coordination bonds.[19] These results further confirmed the successful incorporation of Pd(II) active sites in the PMO–Ph network. This was further confirmed by the TG/DTA analysis. As shown in Fig. 4, besides weight loss due to the removal of physisorbed water, the Pd–PPh$_2$–PMO–Ph sample displayed three exothermic peaks at 611, 673 and 811 K with weight loss around 8.8, 11.2 and 9.2% owing to the subsequent combustions of the PPh$_2$-CH$_2$-CH$_2$-, PPh$_3$- and Ph-groups anchored on the silica support,[20] which was consistent with the weights of these organic groups calculated theoretically.

Figure 5 revealed that both the PPh$_2$–PMO–Ph and the Pd–PPh$_2$–PMO–Ph samples displayed type IV N$_2$ adsorption–desorption isotherms with the H$_1$ hysteresis loop, which was characteristic of typical mesoporous structure.[21] The immobilization of the Pd(II) organometallic catalyst had no significant influence on the shape of the N$_2$ adsorption–desorption isotherm, but caused little decrease in the S_{BET}, D_P and V_P (see Table 1) due to the occupation of the Pd(II) complexes in the pore channels. Meanwhile, the small-angle XRD patterns (Fig. 6) showed three well-resolved peaks indicative of the (100), (111) and (200) diffractions, suggesting the relatively high ordered degree of the mesoporous structure.[22] The TEM images (Fig. 7) further confirmed that both the PPh$_2$–PMO–Ph and the Pd–PPh$_2$–PMO–Ph samples exhib-

ited long-range ordered 2D *p6mm* hexagonal mesoporous channels.[23]

Table 1 summarizes the catalytic parameter of different Pd(II)-based catalysts during water-medium Barbier reaction between benzaldehyde and allyl bromide. The Pd–PPh$_2$–SBA-15–Ph exhibited much higher activity and selectivity than Pd–PPh$_2$–SBA-15, showing the promoting effect of phenyl group. The incorporation of the Ph-groups into the SBA-15 greatly enhanced the surface hydrophobicity, which could promote the adsorption on the catalyst and thus improve both the activity and the selectivity. The Pd–PPh$_2$–PMO–Ph exhibited similar selectivity to the Pd–PPh$_2$–SBA-15–Ph, implying that the nature and the chemical environment of the Pd(II) active sites in these two catalysts were essentially equivalent. However, the Pd–PPh$_2$–PMO–Ph was much more active than the Pd–PPh$_2$–SBA-15–Ph, which could be understood by considering the different ways of Ph-functionalization. The Ph-groups in the Pd–PPh$_2$–PMO–Ph were embedded into the silica walls rather than anchored in the pore channels. However, the Ph-groups in the Pd–PPh$_2$–SBA-15–Ph were occupied the pore channels, leading to an abrupt decrease in S_{BET}, D_P and V_P (see Table 1). Accordingly, the Pd–PPh$_2$–SBA-15–Ph limited the diffusion and adsorption of
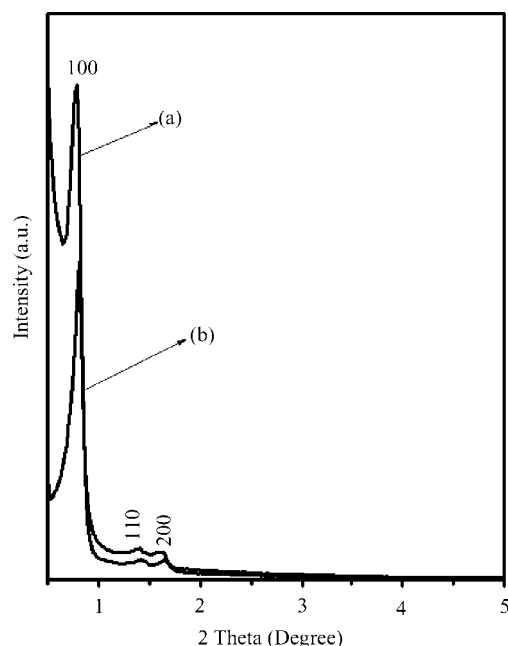
Figure 6. Small angle XRD patterns of (a) PPh$_2$-PMO-Ph and (b) Pd-PPh$_2$-PMO-Ph samples.
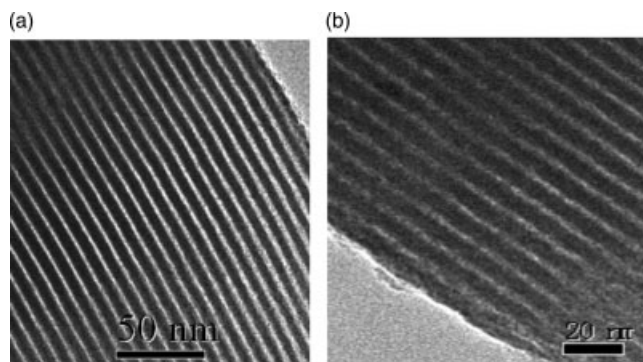

Figure 7. TEM images of (a) PPh$_2$-PMO-Ph and (b) Pd-PPh$_2$-PMO-Ph.

reactant molecules due to steric hindrance, corresponding to the lower activity. The Pd–PPh$_2$–PMO–Ph catalyst was further tested in the Barbier reactions using a different substance (Table 2), which also exhibited matchable activity and selectivity with the Pd(PPh$_3$)$_2$Cl$_2$ homogeneous catalyst. The aliphatic aldehydes and ketones (butyraldehyde, cinnamylaldhyde and acetophenone) were also tested by our catalyst (Pd–PPh$_2$–PMO–Ph); however, the final results showed very poor catalytic performance. The control experiments that were catalyzed by homogeneous catalysts [PdCl$_2$(PPh$_3$)$_2$] displayed similar results, which demonstrated that the above substrate is different to activate in our system. To expand our catalyst application area, we further tested the Pd–PPh$_2$–PMO–Ph catalyst in the water-medium Sonogashira and Heck reactions. As shown in Table 3, the results showed high catalytic efficiency in the two typical carbon–carbon coupling reactions.

To determine whether the heterogeneous or the dissolved homogeneous Pd(II) species were the real catalysts responsible for the allylation reaction between benzaldehyde and allyl bromide, the following procedure was carried out, as proposed
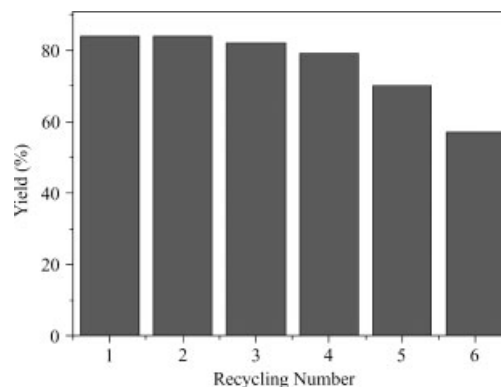

Figure 8. Recycling test of the Pd-PPh$_2$-PMO-Ph catalyst in water-medium Barbier reaction. Reaction conditions are given in Table 1.
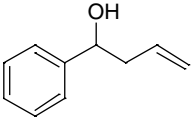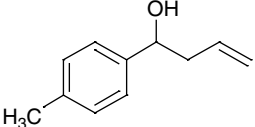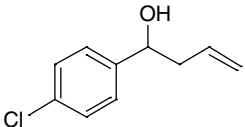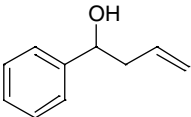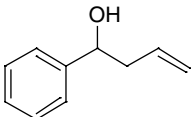
by Sheldon *et al*. When the benzaldehyde conversion reached 30%, the reaction mixture was filtered to remove the solid catalyst and then the mother liquor was allowed to react for another 12 h under the same conditions.[24] No significant change in either the conversion or the yield was observed, indicating that the active phase was not the dissolved Pd(II) species leached from the supports. Therefore it is reasonable to conclude that the present catalysis was really heterogeneous in nature.

The Pd–PPh$_2$–PMO–Ph could be easily separated from the reaction mixture by filtration and used for the subsequent run of reactions. As shown in Fig. 8, the catalyst could be used repetitively five times without significant decrease in the catalytic efficiency. However, further increase in the recycled uses caused an abrupt decrease in the catalytic efficiency. As shown in Table 1, the activity decreased by 20% while the selectivity remained almost unchanged in sixth run of recycled tests. One possible reason was the leach of Pd(II) active sites since the ICP analysis revealed that 3.5% Pd(II) species had leached after reaction six times (see Table 1). Another important reason was damage to ordered mesoporous structure, due to the amphour pore wall of our mesoporous catalyst, which could not stand the hot water over the long running time. As shown in Fig. 9, the Pd–PPh$_2$–PMO–Ph after being used five times displayed a significant deformation of the N$_2$ adsorption–desorption isotherm. Meanwhile, the small-angle XRD patterns in Fig. 10 demonstrated an abrupt decrease in the ordering degree of mesoporous structure. The damage of ordered mesoporous structure caused an abrupt decrease in the S_{BET}, D_P and V_P, which might limit the diffusion of reactant molecules in the pore channels and their adsorption on Pd(II) active sites, leading to a decrease in the catalytic activity.[25]

Conclusions

In summary, this work developed a new approach to designing Pd(II) organometallic catalysts immobilized on the phenyl-functionalized PMO (Pd–PPh$_2$–PMO–Ph). The ordered mesoporous structure ensured the high dispersion of Pd(II) active sites and also diminished the diffusion limit of organic reactant molecules. The phenyl-groups embedded in the silica walls could promote the adsorption of organic molecules on Pd(II) active sites, especially in aqueous solution. As a result, the Pd–PPh$_2$–PMO–Ph exhibited comparable activity and

Table 2. Catalytic performances of the Pd–PPh$_2$–PMO–Ph and Pd(PPh$_3$)$_2$Cl$_2$ in different Barbier reactions[a]
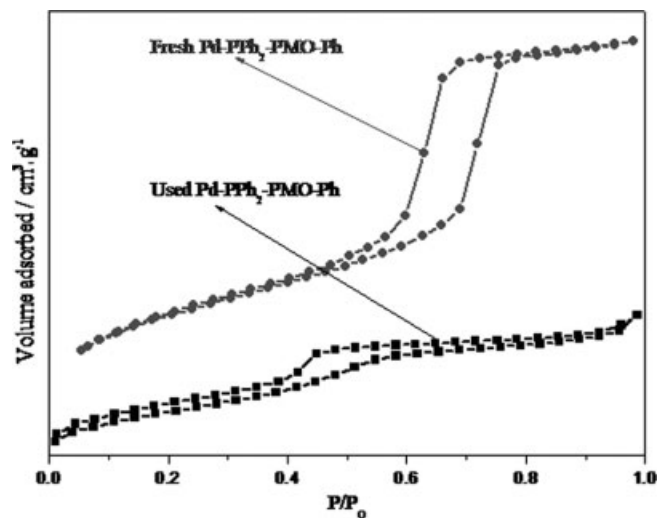
Entry	Catalyst	R	X	Product	Conversion (%)	Selectivity (%)	Yield (%)
1	Pd–PPh$_2$–PMO–Ph	H	Br	1-phenyl-3-buten-1-ol	92	92	84
	Pd(PPh$_3$)$_2$Cl$_2$				96	94	90
2	Pd–PPh$_2$–PMO–Ph	CH$_3$	Br	1-(4-methylphenyl)-3-buten-1-ol	94	78	73
	Pd(PPh$_3$)$_2$Cl$_2$				91	90	82
3	Pd–PPh$_2$–PMO–Ph)	Cl	Br	1-(4-chlorophenyl)-3-buten-1-ol	94	95	89
	Pd(PPh$_3$)$_2$Cl$_2$				99	92	91
4	Pd–PPh$_2$–PMO–Ph	H	Cl	1-phenyl-3-buten-1-ol	89	88	78
	Pd(PPh$_3$)$_2$Cl$_2$				93	96	89
5	Pd–PPh$_2$–PMO–Ph	H	I	1-phenyl-3-buten-1-ol	94	85	80
	Pd(PPh$_3$)$_2$Cl$_2$				98	97	95

[a] Reaction conditions are shown in Table 1.

Table 3. Catalytic performaces of the Pd–PPh$_2$–PMO–Ph catalyst in water-medium Sonogashira and Heck reactions

Entry	R	Sonogashira reaction[a]		Heck reaction[b]	
		Conversion (%)	Yield (%)	Conversion (%)	Yield (%)
1	H	76	74	79	79
2	OCH$_3$	74	73	72	72
3	NO$_2$	79	74	90	90

Reaction conditions: [a] 0.0048 mmol Pd(II), 0.24 mmol phenylacetylene, 0.26 mmol iodobenzene, 0.15 mmol n-decane as internal standard, 0.72 mmol DBU, 5.0 ml distilled water, 0.078 mmol CuI, reaction temperature = 353 K, reaction time = 3 h; [b] 0.0060 mmol Pd(II), 0.20 mmol styrene, 0.24 mmol iodobenzene, 0.40 mmol Et$_3$N, 0.15 mmol n-decane as internal standard, 5.0 ml distilled water, reaction temperature = 353 K, reaction time = 5 h.

Figure 9. N$_2$ adsorption-desorption isotherms of the fresh Pd-PPh$_2$-PMO-Ph and the Pd-PPh$_2$-PMO-Ph after being used repetitively for 5 times.

selectivity with the corresponding PdCl$_2$(PPh$_3$)$_2$ homogeneous catalyst, and could be used repetitively, which could reduce the cost and also diminish the environmental pollution from heavy metallic ions. Other immobilized organometallic catalysts could also be designed based on the present method, which offered more opportunities for clean organic syntheses in water medium.
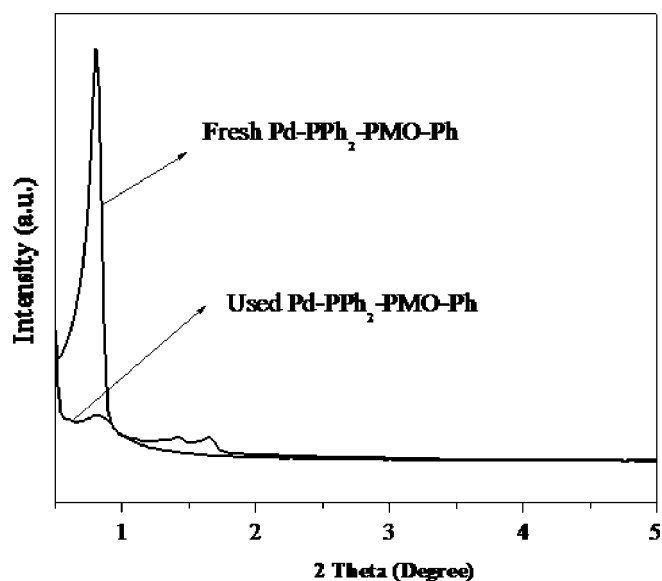
Acknowledgment

Figure 10. Small-angle XRD patterns of the fresh Pd-PPh$_2$-PMO-Ph and the Pd-PPh$_2$-PMO-Ph after being used repetitively for 5 times.

References

[1] A. Schmid, J. S. Dordick, B. Hauer, A. Kiener, M. Wunnolts, B. Witholt, *Nature* **2001**, *409*, 258–268.
[2] R. Sheldon, I. Arends, U. Hanefeld, *Green Chemistry and Catalysis*, Wiley-VCH: Weinheim, Germany, **2007**.
[3] P. A. Grieco, *Organic Synthesis in Water*, Thomson Science: Glasgow, **1998**.
[4] C. J. Li, *Chem. Rev.* **2005**, *105*, 3095–3166.
[5] S. Minakata, M. Komatsu, *Chem. Rev.* **2009**, *109*, 711–724.
[6] C. E. Song, D. H. Kim, D. S. Choi, *Eur. J. Inorg. Chem.* **2006**, *15*, 2927–2935.
[7] H. X. Li, W. Chai, F. Zhang, J. Chen, *Green Chem.* **2007**, *9*, 1223–1228.
[8] N. Gurbuz, I. Özdemir, B. Cetinkaya, T. Seckin, *Appl. Organometal. Chem.* **2003**, *17*, 776–780.
[9] A. F. Grandsire, C. Laborde, F. Lamaty, A. Mehdi, *Appl. Organometal. Chem.* **2010**, *24*, 179–183.
[10] Q. H. Yang, J. Liu, L. Zhang, C. Li, *J. Mater. Chem.* **2009**, *19*, 1945–1955.
[11] J. A. Margolese, S. C. Melero, B. F. Christiansen, G. D. Stucky, *Chem. Mater.* **2000**, *12*, 2448–2459.
[12] Q. Y. Hu, J. E. Hampsey, N. Jiang, C. J. Li, Y. F. Lu, *Chem. Mater.* **2005**, *17*, 1561–1569.
[13] Y. C. Cao, X. Z. Jiang, W. H. Song, Z. Q. Bai, X. Q. Fang, *Catal. Lett.* **2001**, *76*, 53–57.
[14] A. P. H. J. Schenning, A. F. M. Kilbinger, F. Biscarini, M. Cavallini, H. J. Cooper, P. J. Derrick, W. J. Feast, R. Lazzaroni, P. Leclère, L. A. McDonell, E. W. Meijer, S. C. J. Meskers, *J. Am. Chem. Soc.* **2002**, *124*, 1269–1275.
[15] C. M. Li, J. Liu, L. Zhang, J. Yang, Q. H. Yang, *Micro. Meso. Mater.* **2008**, *113*, 333–342.
[16] R. Sayah, M. L. Floch, E. Framery, V. Dufaud, *J. Mol. Catal. A: Chem.* **2010**, *315*, 51–59.
[17] P. F. W. Simon, R. Ulrich, H. W. Spiess, U. Wiesner, *Chem. Mater.* **2001**, *13*, 3464–3486.
[18] T. Posset, F. Rominger, J. Blumel, *Chem. Mater.* **2005**, *17*, 586–595.
[19] J. H. Nelson, J. A. Rahn, W. H. Bearden, *Inorg. Chem.* **1987**, *26*, 2192–2193.
[20] S. Inagaki, S. Guan, T. Ohsuna, O. Terasaki, *Nature* **2002**, *416*, 304–307.
[21] D. Y. Zhao, Q. Huo, J. Feng, B. F. Chmelka, G. D. Stucky, *J. Am. Chem. Soc.* **1998**, *120*, 6024–6036.
[22] O. Muth, C. Schellbach, M. Frvba, *Chem. Commun.* **2001**, *19*, 2032–2033.
[23] G. Fan, S. Cheng, M. Zhu, X. Gao, *Appl. Organometal. Chem.* **2007**, *21*, 670–675.
[24] R. A. Sheldon, M. I. Wallau, W. C. E. Arends, U. Schuchardt, *Acc. Chem. Res.* **1998**, *31*, 485–493.
[25] C. Baleizão, B. Gigante, D. Das, M. Álvaro, H. Garcia, A. Corma, *J. Catal.* **2004**, *223*, 106–113.

773